Journal of the Ceramic Society of Japan 121 [1] 84-88 2013 Paper

Preparation of perovskite-type oxides from heterometal coordination polymer precursors linked by oxalate ligands, $\{Sm[M(ox)_3]\cdot nH_2O\}_x$ (M = Fe or Co)

Syuhei YAMAGUCHI, Naoya KIMOTO, Hirotoshi SASAGAWA, Keiko TAKIGUCHI, Takahisa OKUWA, Makiko ASAMOTO and Hidenori YAHIRO†

Department of Materials Science and Biotechnology, Graduate School of Science and Engineering, Ehime University, Matsuyama 790–8577, Japan

Two kinds of heterometal coordination polymer precursors, $\{Sm[M(ox)_3]\cdot nH_2O\}_x$ (M = Fe and Co), were prepared by the reaction of $K_3[M(ox)_3]\cdot 3H_2O$ with $Sm(NO_3)_3\cdot nH_2O$ in methanol solvent. These compounds were found to have oxalato-bridged network structure. On the other hand, the desired heterometal coordination polymer precursors could not be obtained by the present preparation method using water solvent. The thermal decomposition behaviors of these d-f heterometal coordination polymer precursors were investigated under air atmosphere. The perovskite-type oxides, $SmMO_3$ (M = Fe and Co), were found to form in the temperature range of >600°C. The specific surface area of $SmFeO_3$ powder increased with decreasing calcination temperature of Fe-containing heterometal coordination polymer precursor.

Key-words : Heterometal coordination polymer precursor, Oxalate ligand, Perovskite-type oxide, Specific surface area

[Received August 1, 2012; Accepted November 29, 2012]

1. Introduction

Perovskite-type oxide with general formula, ABO_3, in which A is usually an alkaline earth metal ion or a lanthanoid ion and B is a transition metal ion, is one of the compounds used in the environmental-friendly catalytic systems. The perovskite-type oxides have been reported to exhibit high catalytic activity for oxidations of hydrocarbon[1),2)] and chlorinated volatile organic compounds[3)] and decomposition of NO.[4)–6)] In addition, some perovskite-type oxides have been investigated to be employed as electrode materials for solid oxide fuel cells[7)] and oxygen sensors[8)–10)] and as sensing materials for the detection of humidity,[11),12)] alcohol,[13)] oxygen,[14),15)] CO,[16)–18)] NO_2,[19),20)] and other gases.[21)]

The preparation method of perovskite-type oxide catalyst has been progressively improved. Traditionally, perovskite-type oxides were prepared by solid state reaction of oxides and/or carbonates.[22)–24)] However, the traditional method possesses the disadvantages of long processing time, low surface area, large particle size, and limited degree of chemical homogeneity. Wet-chemical methods are available to prepare finer and more homogeneous powders at low temperature. Up to date, numerous efforts of low temperature wet-chemical method have been undertaken to increase the surface area of perovskite-type oxide. For example, sol–gel,[23),25)–27)] co-precipitation,[22),25),28)] citrate route,[22),23)] reverse micelle,[29),30)] reverse homogeneous precipitation,[31)] and polymeric precursor methods,[32),33)] and flame hydrolysis of aqueous solution of precursor salts[34)] have been developed and designed to prepare nano-sized perovskite-type oxides. However, the development of simple and low-cost procedures for obtaining single-phase perovskite-type oxide nanoparticles with a homogeneous chemical composition under mild condition is still needed.

Sadaoka and co-workers[35)–42)] reported the new preparation route of perovskite-type oxide via the thermal decomposition of heteronulear cyano complex, $Ln[M(CN)_6]\cdot nH_2O$ (abbreviated as CN method). Recently, we have prepared $SmFe_{0.5}Co_{0.5}O_3$ catalyst by CN method and found that this catalyst exhibited the highest CO conversion among a series of $SmFe_xCo_{1-x}O_3$ catalysts due to high homogeneity in composition.[43)] Thus, CN method possesses advantages for preparing perovskite-type oxide active for catalytic CO oxidation; however, there is a serious problem that CN^- group with highly toxic property is containing in starting materials, $K_3[M(CN)_6]$ complexes. Sakamoto and co-workers[44),45)] have succeeded the preparation of perovskite-type oxide using heteronulear oxalato complex precursors, $Ln[Cr(ox)_3]\cdot 10H_2O$ (Ln = La, Pr or Nd) and $La[Co(ox)_3]\cdot 8.5H_2O$ (abbreviated as Ox method). However there is little information about the preparation method of lanthanoid(III)-transition metal(III) coordination polymer linked by oxalate ligands, $Ln[M(ox)_3]\cdot nH_2O$. In this report, the heterometal coordination polymer precursor, $\{Sm[Fe(ox)_3]\cdot 3H_2O\}_x$, was prepared by the reaction of $K_3[Fe(ox)_3]\cdot 3H_2O$ with $Sm(NO_3)_3\cdot nH_2O$ in water or methanol as a solvent, and was characterized by several methods. The obtained $\{Sm[Fe(ox)_3]\cdot 3H_2O\}_x$ precursor was calcined to yield perovskite-type oxide, $SmFeO_3$. In a similar manner, $\{Sm[Co(ox)_3]\cdot 3H_2O\}_x$ precursor was also prepared.

2. Experimental

2.1 Materials and instruments

All chemicals, $Sm(NO_3)_3\cdot 6H_2O$ (Wako, 99.5%), 18-crown-6 (Wako, 98.0%), methanol (Wako, 99.8%), and diethyl ether (Wako, 99.5%), were used as received. Transition metal oxalate potassium salts, such as $K_3[Fe(ox)_3]\cdot 3H_2O$ and $K_3[Co(ox)_3]\cdot 3H_2O$, were synthesized as starting materials according to reported method.[46)]

The powder XRD patterns of the catalysts were collected on a Rigaku MiniFlex II diffractometer using Cu Kα radiation. UV–vis. spectra were recorded on a Hitachi U-4000 spectrometer. The thermal decomposition process of complex was studied by

† Corresponding author: H. Yahiro; E-mail: hyahiro@ehime-u.ac.jp

Table 1. Analytical results of all samples prepared in this work

Sample	Color	Found/wt %[a] (Calcd/wt %)			
		C	Sm	Co	Fe
(i)	White	9.50	34.3	—	N. D
(ii)	Yellow green	15.72	29.6	—	11.9
(iii)	White	9.58	31.7	N. D.	—
(iv)	Green	11.85	23.0	8.6	—
Calculated					
$Sm[Sm(ox)_3]\cdot 12H_2O$		9.23	38.5	—	—
$Sm[Fe(ox)_3]\cdot 3H_2O$		13.74	28.6	—	10.6
$Sm[Co(ox)_3]\cdot 8H_2O$		11.67	24.3	9.5	—

a) ICP and CHN elemental analysis results.

thermogravimetry and differential thermal analysis (TG–DTA; DTG-60E, Shimadzu), performed at a heating rate of 10°C·min^{-1} in air. FT-IR spectra of samples with KBr powder were recorded with a PerkinElmer Spectrum One spectrometer. The specific surface area was determined with the BET analysis (Belsorp-mini, BEL Japan) for the adsorption–desorption property measurements using N_2 adsorbent at −196°C.

2.2 Preparation of complexes

$Sm[Fe(ox)_3]\cdot nH_2O$ was prepared by the similar method reported for $La[Co(ox)_3]\cdot 8.5H_2O$ preparation.[45] In the present study, two different solvents, water and methanol, were used. (i) A yellow-green aqueous solution (10 mL) containing $K_3[Fe(ox)_3]\cdot 3H_2O$ (5.0 mmol) was added to an aqueous solution (10 mL) of $Sm(NO_3)_3\cdot 6H_2O$ (5.0 mmol) under stirring at room temperature. Immediately, white precipitates were formed. After the mixture was further stirred for 4 h, the white precipitates were corrected by suction filtration, washed with water and diethyl ether, and dried in the open air to yield sample (i). (ii) A yellow-green methanol solution (100 mL) containing both $K_3[Fe(ox)_3]\cdot 3H_2O$ (5.0 mmol) and 18-crown-6 (22.7 mmol) was added to a methanol solution (100 mL) of $Sm(NO_3)_3\cdot 6H_2O$ (5.0 mmol) under stirring at room temperature. The role of 18-crown-6 will be discussed later. In this case, yellow-green precipitates were immediately formed. After the mixture was further stirred for 4 h, the precipitates were corrected by suction filtration, washed with water and diethyl ether and dried in vacuum to yield sample (ii).

$Sm[Co(ox)_3]\cdot nH_2O$ was prepared by as-described method of $Sm[Fe(ox)_3]\cdot nH_2O$. In the case of water solvent, the white precipitates [sample (iii)] were obtained. On the other hand, in the case of methanol solvent, the greenish precipitates [sample (iv)] were obtained.

The results of elemental analysis for samples (i–iv) are summarized in **Table 1** as well as color of samples.

2.3 Preparation of perovskite-type oxides with thermal decomposition of precursors

Perovskite-type oxides were prepared by calcining the prepared precursors at desired temperature; the prepared precursors was preheated at 300°C for 1 h and then calcined at 550–1000°C for 24 h in air.

3. Results and discussion

3.1 Preparation and characterization of coordination polymer precursors

Preparation of coordination polymer precursors linked by oxalate ligands, $Sm[M(ox)_3]\cdot nH_2O$, were carried out in water or methanol solvent.

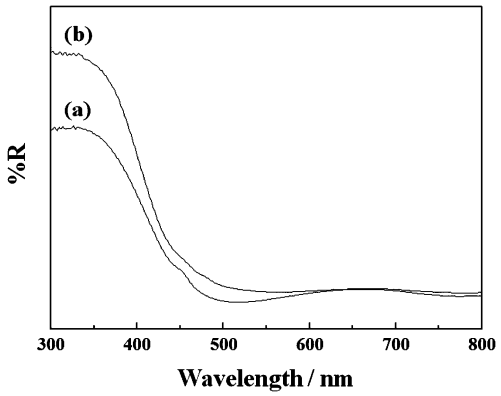

Fig. 1. Diffuse reflectance UV–vis. spectra of sample (ii) (a), and $K_3[Fe(ox)_3]\cdot 3H_2O$ (b).

3.1.1 Water solvent

Nakayama et al.[45] reported that $La[Co(ox)_3]\cdot 8.5H_2O$ could be prepared in water solvent. Therefore, we attempted to prepare $Sm[Fe(ox)_3]\cdot nH_2O$ and $Sm[Co(ox)_3]\cdot nH_2O$ precursors in water solvent [samples (i) and (iii)]. UV–vis. spectra of samples (i) and (iii) exhibited no absorption band of d-d transition or ligand-to-metal charge transfers (LMCT) characteristic for $[M(ox)_3]^{3-}$ frameworks [M = Fe(III) and Co(III)]. The IR spectra of samples (i) and (iii) exhibited the antisymmetric [ν_{as}(CO)] and symmetric ([ν_s(CO)]) vibrations at 1640 and 1363 cm^{-1}, respectively, being in good agreement with those of $Ln[Ln(ox)_3]\cdot 12H_2O$ (Ln = La–Yb, except for Pm) with the respective vibrations at 1686–1560 and 1370 cm^{-1}.[47] Furthermore, the analytical results of samples (i) and (iii), shown in Table 1, demonstrated that the compositions of samples (i) and (iii) were clearly different from those of desired coordination polymer precursors, $Sm[Fe(ox)_3]\cdot nH_2O$ and $Sm[Co(ox)_3]\cdot nH_2O$; the amounts of Fe and Co were below detectable levels for samples (i) and (iii), respectively, and that the compositions of samples (i) and (iii) were roughly consistent with that of $Sm[Sm(ox)_3]\cdot 12H_2O$. Therefore, the samples (i) and (iii) was assigned to $Sm[Sm(ox)_3]\cdot 12H_2O$. These assignments were supported by the following experimental result; when samples (i) and (iii) were calcined at 700°C for 24 h, only XRD peaks assigned to Sm_2O_3 were observed. Thus, the present method with water solvent did not give our desired heterometal coordination polymer precursors linked by oxalate ligands.

3.1.2 Methanol solvent

The starting materials, such as $K_3[M(ox)_3]\cdot 3H_2O$ (M = Fe and Co), are highly soluble in water, but are hardly soluble in methanol. When crown ether, 18-crown-6, was added to methanol solution, such starting materials became soluble in methanol because the $[(18\text{-crown-6})K]^+$ species soluble in methanol may be generated.[48]

Figure 1 shows the diffuse reflectance UV–vis. spectra of sample (ii) and the corresponding starting material ($K_3[Fe(ox)_3]\cdot 3H_2O$). In the UV vis. spectrum of sample (ii), the LMCT band characteristic of $[Fe(ox)_3]^{3-}$ was observed at 300–400 nm, suggesting that the structure of the chromophore, $[Fe(ox)_3]^{3-}$, was maintained in sample (ii). The IR spectrum of sample (ii) exhibited ν_{as}(CO) and ν_s(CO) vibrations at 1624 and 1384 cm^{-1}, respectively, whereas in $K_3[Fe(ox)_3]\cdot 3H_2O$, the respective vibrations were observed at 1675 and 1399 cm^{-1}. From these results, it is presumed for sample (ii) that the networks are constructed by Sm(III)-ox-Fe(III) linkages as reported for $\{NBu_4[CuCr(ox)_3]\}_x$.[49] Furthermore, in contrast to water solvent, the

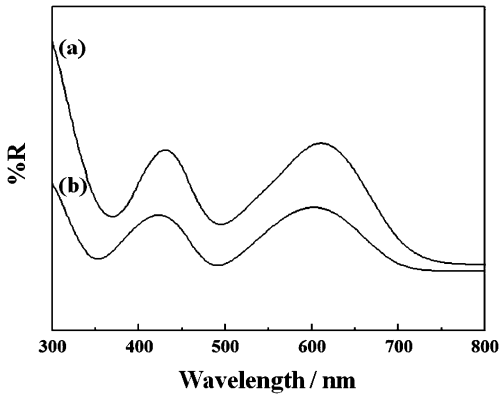

Fig. 2. Diffuse reflectance UV–vis. spectra of sample (iv) (a), and $K_3[Co(ox)_3]\cdot 3H_2O$ (b).

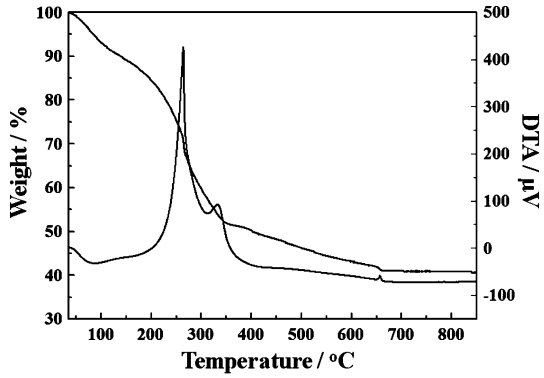

Fig. 3. TG–DTA curves of $Sm[Fe(ox)_3]\cdot nH_2O$.

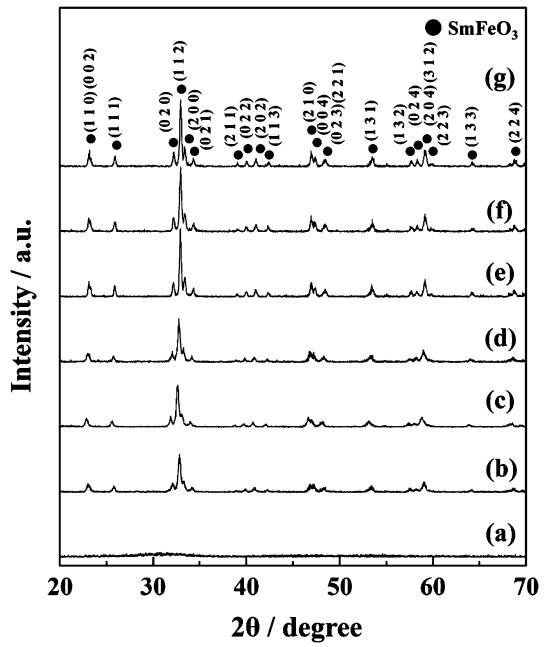

Fig. 4. XRD patterns of $Sm[Fe(ox)_3]\cdot 3H_2O$ calcined at 550 (a), 600 (b), 650 (c), 700 (d), 800 (e), 900 (f), and 1000°C (g).

elemental analysis demonstrated that Sm:Fe:C elemental molar ratio (0.9:1.0:6.1) of sample (ii), calculated from Table 1, was in fair agreement with that of $Sm[Fe(ox)_3]\cdot 3H_2O$ (1:1:6). These results lead us to conclude that $Sm[Fe(ox)_3]\cdot nH_2O$ was formed under the present condition with methanol solvent and that the addition of crown ether to methanol solution makes it possible to prepare the coordination polymer precursor with oxalate ligands, $Sm[Fe(ox)_3]\cdot nH_2O$.

Similarly, sample (iv) was characterized by UV–vis., IR, and elemental analysis. **Figure 2** shows the diffuse reflectance UV–vis. spectra of sample (iv) and $K_3[Co(ox)_3]\cdot 3H_2O$. The d-d bands characteristic of $[Co(ox)_3]^{3-}$ were observed at 434 and 609 nm. In addition, the vibrations of $\nu_{as}(CO)$ and $\nu_s(CO)$ in IR spectrum of sample (iv) were observed at 1624 and 1384 cm^{-1}, respectively. The elemental analysis shown in Table 1 exhibited that Co/Sm weight ratio (Co/Sm molar ratio = 0.95) in sample (iv) agreed with that of that of the calculated value of $Sm[Co(ox)_3]\cdot 8H_2O$. Considering above experimental results, sample (iv) was assigned to $Sm[Co(ox)_3]\cdot nH_2O$.

The sample (iv) gradually changed in color from green to pink under air atmosphere. This change may be due to the decomposition of oxalate ligands in $Sm[Co(ox)_3]\cdot nH_2O$, accompanying with the reduction from Co(III) to Co(II). A similar change in color has been already reported for the reformation of $La[Co(ox)_3]\cdot 8.5H_2O$ to $1/2La_2(C_2O_4)_3$ and CoC_2O_4.[45] Thus, $Sm[Co(ox)_3]\cdot nH_2O$ was unstable under air, but comparatively stable under a vacuum condition.

3.2 Thermal decomposition of coordination polymer precursors with oxalate ligands

The thermal decomposition behaviors of samples (ii) and (iv), assigned to $Sm[Fe(ox)_3]\cdot nH_2O$ and $Sm[Co(ox)_3]\cdot nH_2O$, respectively, in section 3.1, were investigated in order to prepare the perovskite-type oxides, $SmFeO_3$ and $SmCoO_3$, respectively.

TG–DTA curve of $Sm[Fe(ox)_3]\cdot nH_2O$ is shown in **Fig. 3**. The decomposition started at about 50°C to give the first plateau in the temperature range of 100 to 200°C. The weight loss percentage in this plateau range was about 12%, indicating the formation of anhydrate species, $\{Sm[Fe(ox)_3]\}_x$. This weight loss corresponds to that of about 3 crystallization water molecules; namely the n value in $Sm[Fe(ox)_3]\cdot nH_2O$ was found to be 3. With further increasing temperature, the abrupt weight loss accompanying with large exothermic DTA peak was observed at ca. 270°C to give the second plateau. It is suggested that this weight loss is attributable to the oxidation of oxalate ligands. After gradual decrease in weight, probably due to the desorption of CO_2 from oxidative products formed on sample, and the third plateau appeared at above 650°C. The total weight loss percentage (ca. 59%) of sample (ii) was consistent with the calculated one (57%) by assuming the formation to $SmFeO_3$ from $Sm[Fe(ox)_3]\cdot 3H_2O$.

The decomposition product of $Sm[Fe(ox)_3]\cdot 3H_2O$ was characterized by measuring the powder X-ray diffraction spectrum of the product calcined at 550, 600, 650, 700, 800, 900, and 1000°C for 24 h under air. The XRD results are shown in **Fig. 4**. The perovskite-type oxide, $SmFeO_3$, was formed at >600°C and no peak attributable to Sm_2O_3 and Fe_2O_3 was observed. The crystal system and space group of sample calcined at 700°C were orthorhombic and *Pbnm*, respectively, and the lattice constants (Å) were estimated as follows: $a = 5.425$, $b = 5.609$, $c = 7.622$ Å. The average sizes of the $SmFeO_3$ crystallites in the (110) direction, evaluated from XRD line broadening using Scherrer's equation, are shown in **Table 2**. The evaluated values decreased with decreasing calcination temperature of a heterometal coordination polymer precursor. BET specific surface areas of the $SmFeO_3$ samples calcined at each temperature are also shown in Table 2. The specific surface areas increased with decreasing calcination temperature. The specific surface area of

Table 2. Average sizes of crystallite and specific surface areas of products calcined at each temperature

Sample	Calc. Temp. /°C	Crystallite size /nm[a)]	Surface area /$m^2 \cdot g^{-1}$
(ii)	550	—[b)]	—[c)]
	600	22	8.6
	650	23	—[c)]
	700	25	7.9
	800	27	3.3
	900	29	—[c)]
	1000	31	1.8
(iv)	700	36	3.9

a) The average sizes of $SmFeO_3$ and $SmCoO_3$ crystallites in the (110) and (002) directions, respectively, were evaluated from XRD line broadening using Scherrer's equation. b) No peaks. c) Not measured.

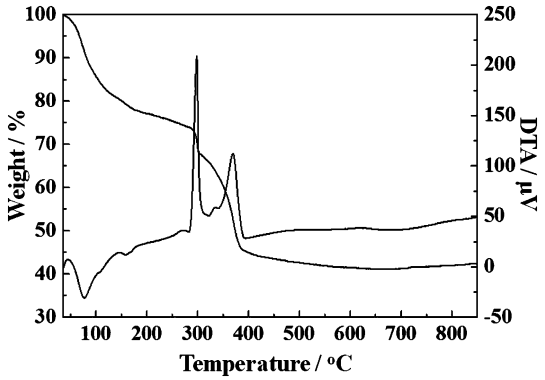

Fig. 5. TG–DTA curves of $Sm[Co(ox)_3]\cdot nH_2O$.

the $SmFeO_3$ powder calcined at 600°C was 8.6 $m^2 \cdot g^{-1}$, being comparable to that of the $SmFeO_3$ powder prepared by CN method (ca. 9 $m^2 \cdot g^{-1}$).[50)]

The decomposition behavior of $Sm[Co(ox)_3]\cdot nH_2O$ was essentially the same as that of $Sm[Fe(ox)_3]\cdot nH_2O$. TG–DTA curve of $Sm[Co(ox)_3]\cdot nH_2O$ is shown in **Fig. 5**. The decomposition of $Sm[Co(ox)_3]\cdot nH_2O$ started at about 50°C. Similar to $Sm[Fe(ox)_3]\cdot nH_2O$, three steps of weight losses were observed at 50–200 (percentage of weight loss = 23%), 200–380 (31%), and 380–600°C (3%), and the total weight loss percentage was 57%. These results suggest that the decomposition of $Sm[Co(ox)_3]\cdot 8H_2O$ to $SmCoO_3$ through anhydrate species, $\{Sm[Co(ox)_3]\}_x$ successively occurred. **Figure 6** shows the XRD pattern of $Sm[Co(ox)_3]\cdot 8H_2O$ calcined at 700°C for 24 h. Clearly, the single phase $SmCoO_3$ was formed with crystal system: orthorhombic, space group: *Pbnm*, and the lattice constants: $a = 5.307$, $b = 5.305$, and $c = 7.549$ Å.

TG–DTA and XRD measurements demonstrated that the d-f heterometal coordination polymer complex linked by oxalate ligands, $Sm[M(ox)_3]\cdot nH_2O$ (M = Fe and Co) is a potential candidate of precursor to give the perovskite-type oxide, $SmMO_3$, by calcination at relatively low temperature (>600°C).

4. Conclusion

The f-d heteronulear oxalato complex, $\{Sm[M(ox)_3]\cdot nH_2O\}_x$ (M = Fe and Co), with the network structures constructed by Sm(III)-ox-M(III) linkages was prepared as a precursor of perovskite-type oxide with high surface area. The thermal decomposition behavior of the resulting precursor was examined. The obtained results are summarized as follows.

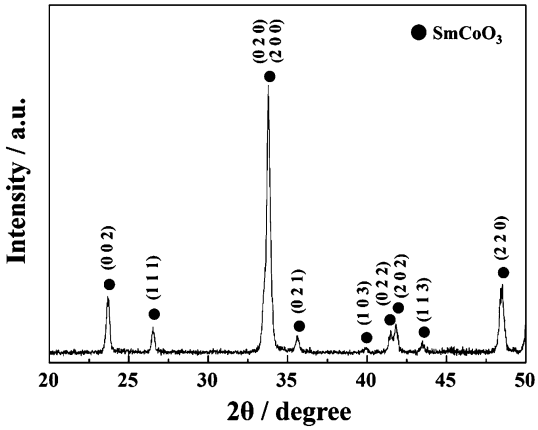

Fig. 6. XRD pattern of $Sm[Co(ox)_3]\cdot 8H_2O$ calcined at 700°C.

(1) Two kinds of f-d heterometal coordination polymer precursors, $Sm[M(ox)_3]\cdot nH_2O$ (M = Fe and Co), were prepared by the reaction of $K_3[M(ox)_3]\cdot 3H_2O$ with $Sm(NO_3)_3\cdot nH_2O$ in methanol solvent containing crown ether, 18-crown-6.
(2) Perovskite-type oxides were formed by calcining $Sm[M(ox)_3]\cdot nH_2O$ precursors at 600°C.
(3) The average crystallite size and the specific surface area of perovskite-type oxide decreased with decreasing calcination temperature of a heterometal coordination polymer precursor. The specific surface area of $SmFeO_3$ powder prepared by Ox method (calcination temperature = 600°C) was 8.6 $m^2 \cdot g^{-1}$, which was comparable to that of $SmFeO_3$ prepared by CN method at same temperature (ca. 9 $m^2 \cdot g^{-1}$).

Acknowledgement This work was supported by JSPS KAKENHI Grant Number 21360397 and 24560948.

References

1) D. W. Johnson, Jr., P. K. Gallagher, G. K. Wertheim and E. M. Vogel, *J. Catal.*, 48, 87–97 (1977).
2) H. Yasuda, Y. Fujiwara, N. Mizuno and M. Misono, *J. Chem. Soc., Faraday Trans.*, 90, 1183–1189 (1994).
3) B. P. Barbero, J. A. Gamboa and L. E. Cadús, *Appl. Catal., B*, 65, 21–30 (2006).
4) Y. Teraoka, H. Fukuda and S. Kagawa, *Chem. Lett.*, 19, 1–4 (1990).
5) Y. Teraoka, K. Nakano, W. Shangguan and S. Kagawa, *Catal. Today*, 27, 107–113 (1996).
6) H. Dai, H. He, P. Li, L. Gao and C.-T. Au, *Catal. Today*, 90, 231–244 (2004).
7) N. Q. Minh, *J. Am. Ceram. Soc.*, 76, 563–588 (1993).
8) T. Inoue, N. Seki, K. Eguchi and H. Arai, *J. Electrochem. Soc.*, 137, 2523–2527 (1990).
9) C. B. Alcock, R. C. Doshi and Y. Shen, *Solid State Ionics*, 51, 281–289 (1992).
10) P. Shuk, A. Vecher, V. Kharton, L. Tichonova, H. D. Wiemhöfer, U. Guth and W. Göpel, *Sens. Actuators, B*, 16, 401–405 (1993).
11) Y. Shimizu, M. Shimabukuro, H. Arai and T. Seiyama, *Chem. Lett.*, 14, 917–920 (1985).
12) J. P. Lukaszewicz, *Sens. Actuators, B*, 4, 227–232 (1991).
13) H. Obayashi and T. Kudo, *Nippon Kagaku Kaishi*, 1980, 1568–1572 (1980).
14) C. Yu, Y. Shimizu and H. Arai, *Chem. Lett.*, 15, 563–566 (1986).

15) M. L. Post, B. W. Sanders and P. Kennepohl, *Sens. Actuators, B*, 13, 272–275 (1993).
16) W. B. Li, H. Yoneyama and H. Tamura, *Nippon Kagaku Kaishi*, 1982, 761–767 (1982).
17) Y. Takahashi and H. Taguchi, *J. Mater. Sci. Lett.*, 3, 251–252 (1984).
18) T. Arakawa, K. Takada, Y. Tsunemine and J. Shiokawa, *Sens. Actuators*, 14, 215–221 (1988).
19) Y. Matsuura, S. Matsushima, M. Sakamoto and Y. Sadaoka, *J. Mater. Chem.*, 3, 767–769 (1993).
20) E. Traversa, S. Matsushima, G. Okada, Y. Sadaoka, Y. Sakai and K. Watanabe, *Sens. Actuators, B*, 25, 661–664 (1995).
21) T. Arakawa, H. Kurachi and J. Shiokawa, *J. Mater. Sci.*, 4, 1207–1210 (1985).
22) S. Royer, F. Bérubé and S. Kaliaguine, *Appl. Catal., A*, 282, 273–284 (2005).
23) R. J. Bell, G. J. Millar and J. Drennan, *Solid State Ionics*, 131, 211–220 (2000).
24) K. Rida, A. Benabbas, F. Bouremmad, M. A. Peña and A. Martínez-Arias, *Catal. Commun.*, 7, 963–968 (2006).
25) P. V. Gosavi and R. B. Biniwale, *Mater. Chem. Phys.*, 119, 324–329 (2010).
26) H. M. Zhang, Y. Teraoka and N. Yamazoe, *Chem. Lett.*, 16, 665–668 (1987).
27) K. Rida, A. Benabbas, F. Bouremmad, M. A. Peña, E. Sastre and A. Martínez-Arias, *Appl. Catal., A*, 327, 173–179 (2007).
28) W. Li, M. W. Zhou and J. L. Shi, *Mater. Lett.*, 58, 365–368 (2004).
29) M. Yuasa, K. Shimanoe, Y. Teraoka and N. Yamazoe, *Catal. Today*, 126, 313–319 (2007).
30) A. E. Giannakas, A. A. Leontiou, A. K. Ladavos and P. J. Pomonis, *Appl. Catal., A*, 309, 254–262 (2006).
31) Y. Teraoka, S. Nanri, I. Moriguchi, S. Kagawa, K. Shimanoe and N. Yamazoe, *Chem. Lett.*, 29, 1202–1203 (2000).
32) K. Tsuchida, S. Takase and Y. Shimizu, *Sens. Mater.*, 16, 171–180 (2004).
33) M. Popa, J. Frantti and M. Kakihara, *Solid State Ionics*, 154–155, 437–445 (2002).
34) I. Rossetti and L. Forni, *Appl. Catal., B*, 33, 345–352 (2001).
35) Y. Matsuura, S. Matsushima, M. Sakamoto and Y. Sadaoka, *J. Mater. Chem.*, 3, 767–769 (1993).
36) Y. Sadaoka, E. Traversa and M. Sakamoto, *Chem. Lett.*, 25, 177–178 (1996).
37) Y. Sadaoka, E. Traversa and M. Sakamoto, *J. Alloys Compd.*, 240, 51–59 (1996).
38) M. Sakamoto, P. Nunziante, E. Traversa, S. Matsushima, M. Miwa, H. Aono and Y. Sadaoka, *J. Ceram. Soc. Japan*, 105, 693–696 (1997).
39) E. Traversa, P. Nunziante, M. Sakamoto, Y. Sadaoka, M. C. Carotta and G. Martinelli, *J. Mater. Res.*, 13, 1335–1344 (1998).
40) E. Traversa, P. Nunziante, M. Sakamoto, Y. Sadaoka and R. Montanari, *Mater. Res. Bull.*, 33, 673–681 (1998).
41) Y. Sadaoka, H. Aono, E. Traversa and M. Sakamoto, *J. Alloys Compd.*, 278, 135–141 (1998).
42) H. Aono, M. Sato, E. Traversa, M. Sakamoto and Y. Sadaoka, *J. Am. Ceram. Soc.*, 84, 341–347 (2001).
43) M. Asamoto, N. Harada, Y. Iwamoto, H. Yamaura and H. Yahiro, *Top. Catal.*, 52, 823–827 (2009).
44) M. Sakamoto, K. Matsuki, R. Ohsumi, Y. Nakahama, Y. Sadaoka, S. Nakayama, N. Matsumoto and H. Okawa, *J. Ceram. Soc. Japan*, 100, 1211–1215 (1992).
45) S. Nakayama, M. Okazaki, Y. L. Aung and M. Sakamoto, *Solid State Ionics*, 158, 133–139 (2003).
46) J. C. Bailar, Jr. and E. M. Jones, *Inorg. Synth.*, 1, 35–38 (1939).
47) D. Kustaryono, N. Kerbellec, S. Calvez, S. Freslon, C. Daiguebonne and O. Guillou, *Cryst. Growth Des.*, 10, 775–781 (2010).
48) W.-H. Yu, X.-Z. Wang, Y.-X. Sui, X.-M. Ren and Q.-J. Meng, *Inorg. Chem. Commun.*, 11, 799–801 (2008).
49) Z. Zhong, N. Matsumoto, H. Okawa and S. Kida, *Chem. Lett.*, 19, 87–90 (1990).
50) M. Asamoto and H. Yahiro, *Catal. Surv. Asia*, 13, 221–228 (2009).